Chinese Chemical Letters 36 (2025) 110503

Contents lists available at ScienceDirect

Chinese Chemical Letters

journal homepage: www.elsevier.com/locate/cclet

Synthesis of organoboron compounds *via* heterogeneous C–H and C–X borylation

Shuai Tang[1], Zian Wang[1], Mengyi Zhu, Xinyun Zhao*, Xiaoyun Hu*, Hua Zhang*

Key Laboratory of Catalysis and Energy Materials Chemistry of Ministry of Education & Hubei Key Laboratory of Catalysis and Materials Science & Key Laboratory of Analytical Chemistry of the State Ethnic Affairs Commission, School of Chemistry and Materials Science, South-Central Minzu University, Wuhan 430074, China

ARTICLE INFO

Article history:
Received 29 May 2024
Revised 13 September 2024
Accepted 24 September 2024
Available online 24 September 2024

Keywords:
Organoboron compounds
Heterogeneous catalysis
C–H borylation
C–X borylation
Heterogeneous catalysts

ABSTRACT

Homogeneous C–H and C–X borylation *via* transition-metal-catalysis have undergone rapid development in the past decades and become one of the most practical methods for the synthesis of organoboron compounds. However, the catalysts employed in homogeneous catalysis are generally expensive, sensitive, and difficult to separate from the reaction mixture and reuse. With the rapid development of heterogeneous catalysis, heterogeneous C–H and C–X borylation have emerged as highly efficient and sustainable approaches towards the synthesis of organoboron compounds. This review aims to highlight the recent advances in the synthesis of organoboron compounds employing heterogeneous C–H and C–X borylation strategies. We endeavor to shed light on new perspectives and inspire further research and applications in this emerging area.

1. Introduction

Organoboron compounds are valuable building blocks in organic synthesis and have been widely applied in various areas, such as pharmaceutical science and materials science [1-5]. The development of practical and convenient protocols for the synthesis of organoboron compounds has always been one of the core topics of organoboron chemistry. Traditional synthetic routes of organoboron compounds mainly rely on nucleophilic reactions of boron precursors with highly reactive organolithium or Grignard reagents, which suffered from poor functional group tolerance and harsh conditions. Since the pioneering work by Miyaura and Masuda [6,7], numerous transition-metal-catalyzed C–X (X = halide or pseudohalide) borylation transformations have been developed for the efficient access of organoboron compounds [8-11]. Meanwhile, pioneered by Marder and Hartwig [12,13], tremendous efforts have been devoted to transition-metal-catalyzed C–H borylation transformations to convert C–H bonds to C–B bonds [14-20]. Despite significant progress has been made in homogeneous C–H and C–X borylation, difficulties associated with separating the catalyst from the reaction mixture and recovering the catalyst for reuse as well as contamination by toxic metals and the generally high cost and instability of catalyst are notable disadvantages of homogeneous catalysis, which hampers its wider application in chemical and pharmaceutical processes. Therefore, the development of promising approaches to overcome these limitations is highly demanded.

Heterogeneous catalysis is a sustainable alternative to homogeneous approaches for organic transformations, as it can reduce the cost of catalysts, simplify the separation process, and enable large-scale industrial production [21]. These features make it possible to synthesize valuable chemicals on a practical scale in a green manner. In recent years, with the rapid development of sustainable chemistry and heterogeneous catalysis, heterogeneous C–H and C–X borylation have emerged as highly efficient and sustainable approaches towards the synthesis of organoboron compounds (Scheme 1). In this review, we seek to showcase the recent advances in heterogeneous C–H and C–X borylation to synthesize organoboron compounds, which are organized by catalyst support classes in heterogeneous C–H borylation and catalyst classes in heterogeneous C–X borylation. We hope that this review will be helpful in inspiring further advances in this emerging area.

2. Heterogeneous C–H borylation

2.1. Carbon material-supported metal catalyst

The first example of heterogeneous C–H borylation was reported by Miyaura and co-workers in 2001, who achieved the sim-

* Corresponding authors.
E-mail addresses: ccnuzhao@mail.scuec.edu.cn (X. Zhao), xyhu@mail.scuec.edu.cn (X. Hu), huazhang@scuec.edu.cn (H. Zhang).
[1] These authors contributed equally to this work.

https://doi.org/10.1016/j.cclet.2024.110503
1001-8417/

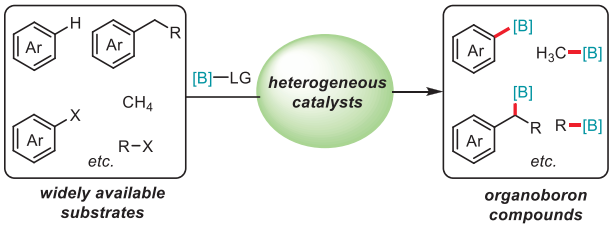

Scheme 1. Synthesis of organoboron compounds *via* heterogeneous C–H and C–X borylation.

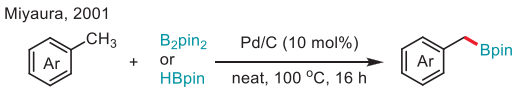

Scheme 2. Pd/C-catalyzed benzylic C–H borylation of alkylbenzenes.

ple Pd/C-catalyzed benzylic C–H borylation of alkylbenzenes to afford pinacol benzylboronates in good yields (Scheme 2) [22]. Other heterogeneous catalysts such as Pt/C, Rh/C, and Ru/C were totally ineffective. The reactions were carried out with B_2pin_2 or HBpin as the limiting reagent in the presence of excessive alkylbenzenes under neat conditions. This catalytic system is highly sensitive to the presence of heteroatom, thus both 4-methyl anisole and 2-methyl thiophene were unsuccessful substrates.

2.2. Silica-supported metal catalysts

Silica is one of the most well-known supports for catalytically active metal complexes especially in C–H borylation [23]. Based on their previously developed Silica-SMAP, a silica-supported, caged, compact monodentate alkylphosphine ligand, in 2009, Sawamura and co-workers prepared Silica-SMAP-Ir *in situ* from $[Ir(OMe)(cod)]_2$ and Silica-SMAP. This silica-supported compact phosphine-iridium system showed high activities for the *ortho*-selective aromatic C–H borylation of arenes with various directing groups, such as ester, amide, sulfonate, acetal, alkoxymethyl, and chlorine groups, under mild reaction conditions (Scheme 3a) [24]. Remarkably, when the reaction of methyl benzoate with B_2pin_2 was carried out under neat conditions at 100 °C on a 20 mmol scale, the Silica-SMAP–Ir exhibited a high turnover number (20,000) while retaining perfect ortho selectivity. By using the same Silica-SMAP–Ir system, they also achieved the site-selective C(sp^3)–H borylation of 2-alkylpyridines (Scheme 3b) [25], site- and stereo-selective C–H borylation of cyclopropanes and cyclobutanes (Scheme 3c) [26], and C8-selective C–H borylation of quinoline derivatives (Scheme 3d) [27]. Very recently, Al Mamari and co-workers reported a method for C8-selective C–H borylation of 4-quinolones using a similar catalytic system (Scheme 3e). The Silica-SMAP–Ir catalyst was easily separated from the products through Celite filtration, but efforts to reuse the catalyst were not successful.

By employing Silica-SMAP-Rh, prepared *in situ* from Silica-SMAP and $[Rh(OH)(cod)]_2$, in 2011, Sawamura and co-workers achieved the *ortho*-selective C–H borylation for a variety of arenes containing nitrogen-based directing groups including *N*-heterocycles, *tert*–aminoalkyl groups, and imine-type groups (Scheme 4a) [29]. Notably, this heterogenous Rh catalysis complements their previously reported heterogenous Ir-catalyzed *ortho*-borylation, which is effective for arenes with oxygen-based directing groups. By using a heterogeneous catalyst system consisting of $[Rh(OMe)(cod)]_2$ and a silica-supported triarylphosphine ligand (Silica-TRIP) featuring an immobilized triptycene-type cage structure with a bridgehead P atom, the site-selective C(sp^3)–H borylation of amides, ureas, and 2-aminopyridine derivatives was realized by the same group (Scheme 4b) [30]. A silica-supported tripod triarylphosphane (Silica-3p-TPP) containing a triphenylphosphane-type core tripodally immobilized on the silica surface was also reported by the same group and employed in the heterogeneous rhodium- and iridium-catalyzed C(sp^3)–H borylation of amide, urea and alkylpyridine derivatives (Scheme 4c) [31]. All these heterogeneous catalysts could be easily separated from the products by Celite filtration but could not be reused.

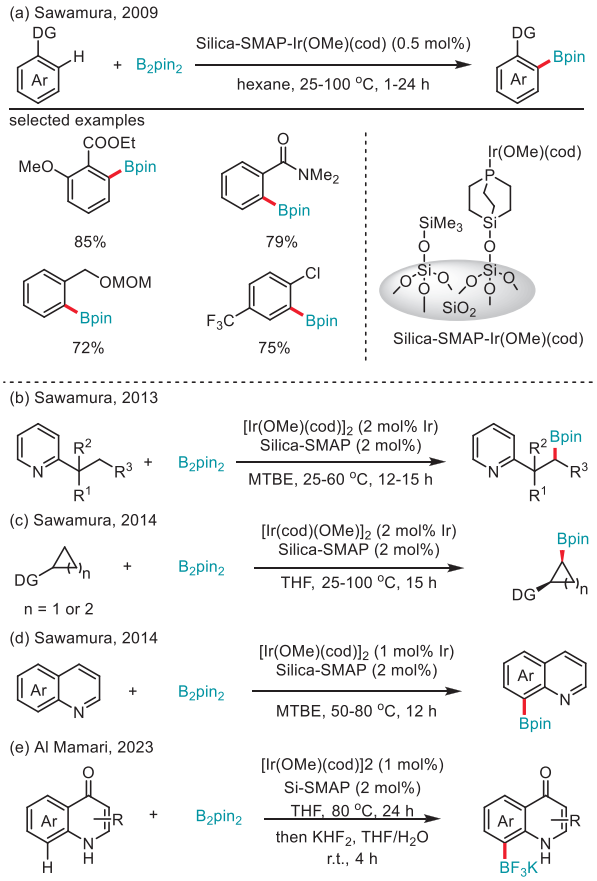

Scheme 3. Silica-SMAP-Ir-catalyzed aromatic C–H borylation of arenes with various directing groups, quinoline, 4-quinolones, and C(sp^3)–H borylation of 2-alkylpyridines, cyclopropanes, and cyclobutanes.

Besides phosphine ligand, bipyridine ligand could also be immobilized on the silica support. In 2014, Jones and co-workers reported that mesoporous silica (SBA-15)-supported bipyridine iridium complex, which was prepared from the SBA-15-supported bipyridine ligand and $[Ir(cod)(OMe)]_2$, exhibited moderate to good catalytic activity for the C–H borylation of various disubstituted arenes (Scheme 5) [32]. Importantly, this heterogeneous catalyst could be recovered easily and reused repeatedly by simple washing without chemical treatment and exhibits good recycling performance with a modest decrease in the catalytic rate over three runs.

In a parallel study to the work of Jones, Inagaki, and co-workers reported the synthesis of BPy-PMO, a periodic mesoporous organosilica (PMO) containing 2,2′-bipyridine (bpy) within the framework (Scheme 6a) [33]. BPy-PMO exhibited excellent ligand properties for the heterogeneous Ir-catalyzed C–H borylation of both electron-rich and -poor substituted arenes with B_2pin_2. This Ir-BPy-PMO catalyst could be easily recovered by simple filtration and retain good catalytic activity with a slight loss of product yield for at least three cycles. A hot-filtration experiment and the subsequent ICP analysis clearly indicated that the catalytic reaction

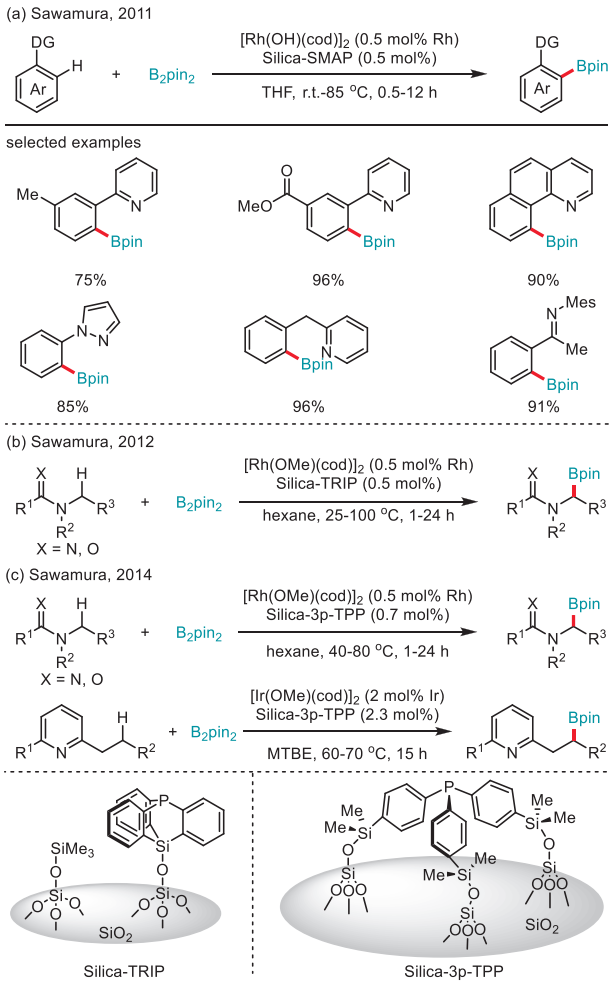

Scheme 4. Silica-SMAP-Rh- and Silica-TRIP-Rh-catalyzed C–H borylation of arenes and Silica-3p-TPP-Rh- and Silica-3p-TPP-Ir-catalyzed C(sp^3)–H borylation of amide, urea and alkylpyridine derivatives.

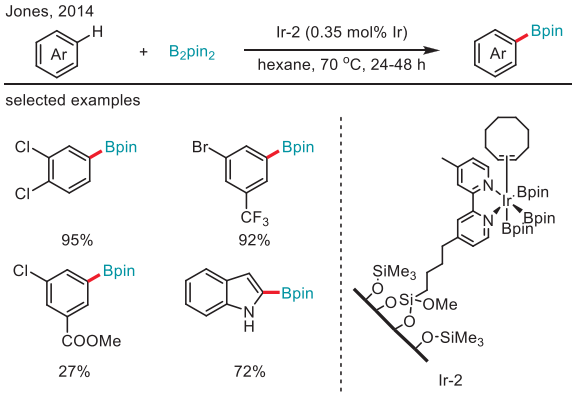

Scheme 5. Ir-2-catalyzed aromatic C–H borylation of arenes.

occurred by the iridium complex fixed on BPy-PMO without leaching of Ir species. In the following year, the same group reported that Ir-BPy-PMO showed high catalytic activity for the C–H borylation of a wide range of arenes and heteroarenes using HBpin as the borylating reagent (Scheme 6b) [34]. Successive recycling reactions could be conducted under similar conditions at least 3 times, although both the reaction rate and product yield gradually declined. By employing a similar strategy, Copéret and co-workers independently reported the synthesis of Ir-bpy$^{1/10}$-PMO, a molecularly de-

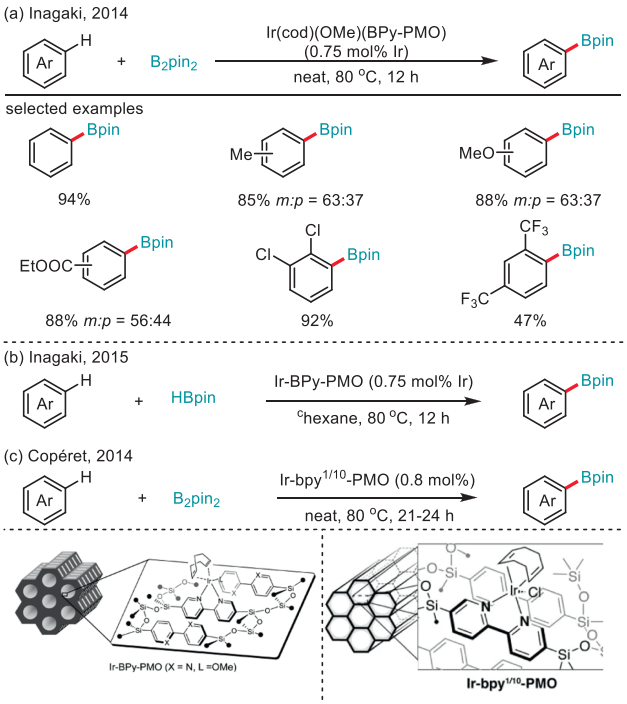

Scheme 6. Ir-BPy-PMO- and Ir-bpy$^{1/10}$-PMO-catalysed aromatic C–H borylation of arenes. Reproduced with permission [34]. Copyright 2015, the Royal Society of Chemistry. Reproduced with permission [35]. Copyright 2014, John Wiley and Sons.

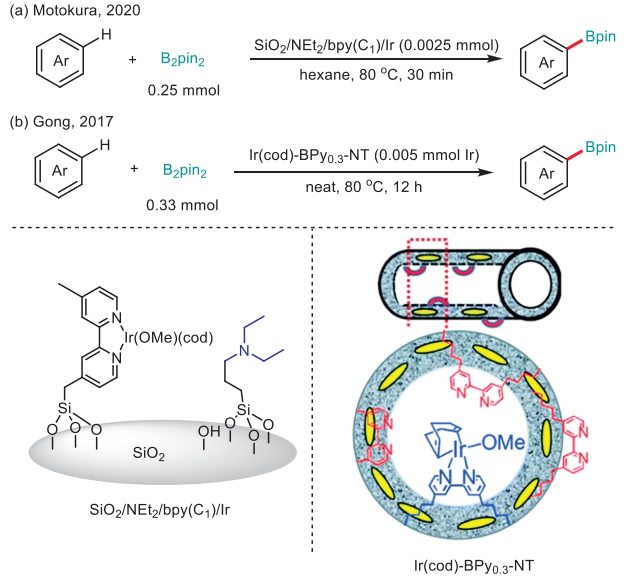

Scheme 7. SiO_2/NEt_2/bpy(C1)/Ir- and Ir(cod)-$BPy_{0.3}$–NT-catalysed aromatic C–H borylation of arenes. Reproduced with permission [37]. Copyright 2017, the Royal Society of Chemistry.

fined Ir(I) catalyst with a PMO containing bipyridylene moieties in a matrix of biphenylene units as ligand platform (Scheme 6c) [35]. This heterogeneous catalyst displayed good catalytic performance for the C–H borylation of benzene, toluene, and anisole, and can be reused without significant loss of activity.

Based on the previous studies of silica-supported Ir-catalysed aromatic C–H borylation, Motokura, and co-workers developed a novel kind of silica-supported Ir catalysts, in which Ir-bipyridine complex and organic functionalities are coimmobilized on the silica surface (Scheme 7a) [36]. They found that the linker length of the Ir–bipyridine complex, the coimmobilized organic functional-

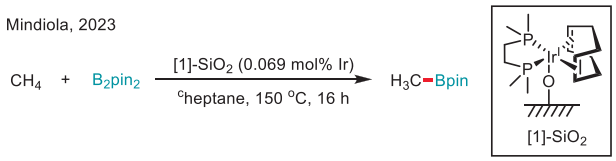

Scheme 8. [1]-SiO_2-catalysed C–H borylation of methane.

ity, and the substituents on the arene substrates significantly affected the catalytic activity for the aromatic C–H borylation. One of the catalysts SiO_2/NEt_2/bpy(C1)/Ir could be recycled at least three times with gradually decreased reaction rate and product yield.

In 2017, Gong and co-workers reported the synthesis of BPy-NT, a one-dimensional organosilica nanotubes containing bipyridine ligands in the framework (Scheme 7b) [37]. The metalation of BPy-NT with $[IrCp^*Cl(\mu\text{-}Cl)]_2$ and $[Ir(cod)(OMe)]_2$ afforded robust heterogeneous catalysts, $IrCp^*$-BPy-NT and Ir(cod)-BPy-NT, which exhibited high catalytic activities for the C–H borylation of arenes. Benefiting from the isolated active sites as well as the fast transport of substrates and products, these nanotube catalysts displayed enhanced activities and durability as compared to the analogous homogeneous catalysts and other conventional heterogeneous catalysts. Notably, the total TONs for Ir(cod)-$BPy_{0.3}$–NT after the 10^{th} reuse could reach up to 900 for benzene borylation.

Since the initial reports by Mindiola and Sanford [38,39], catalytic C–H borylation of the most abundant hydrocarbon, methane (CH_4), has garnered significant interest in recent years. In 2023, Mindiola and co-workers developed a heterogeneous Ir catalyst *via* the surface immobilization of a bisphosphine molecular precatalyst, [(dmpe)Ir(cod)CH_3], onto amorphous silica, which enhanced its performance over 12-fold (Scheme 8) [40]. Impressively, this catalyst [1]-SiO_2 afforded over 2000 turnovers at 150 °C in 16 h with a selectivity of 91.5% for mono- vs diborylation. The supported precatalyst was identified as an Ir^I species and multinuclear Ir polyhydrides were not formed upon completion of catalysis, which revealed that the immobilization of the organometallic Ir species on a surface prevents bimolecular decomposition pathways.

2.3. MOFs-supported metal catalysts

Metal–organic frameworks (MOFs) have attracted increasing interest in recent years as a new class of porous molecular materials for catalyst support in C–H borylation transformations [41]. In 2014, Lin and co-workers reported a highly stable and recyclable single-site heterogeneous Ir catalyst, bpy-UiO-Ir, which was prepared *via* postsynthetic metalation of the 2,2′-bipyridyl-derived metal–organic framework of the UiO (Universitetet i Oslo) structure (bpy-UiO) with $[Ir(COD)(OMe)]_2$ (Scheme 9a) [42]. Bpy-UiO was synthesized *via* a solvothermal reaction between $ZrCl_4$ and 2,2′-bipyridine-5,5′-dicarboxylic acid in the presence of DMF and trifluoroacetic acid. The bpy-UiO-Ir is a highly active catalyst for the C–H borylation of a wide range of activated and unactivated arenes, including halogenated-, alkyl-, and alkoxy-arenes using B_2pin_2. The higher activity of bpy-UiO-Ir as compared to the analogous homogeneous catalyst $[(CO_2Me)_2bpy]Ir(COD)(OMe)$ is likely due to the active site isolation which prevents any intermolecular deactivation pathways. Impressively, at a 2 mol% catalyst loading, bpy-UiO-Ir could be recovered and reused for the borylation of *m*-xylene at least 20 times without significant loss of catalytic activity or MOF crystallinity. In addition, the heterogeneous nature of bpy-UiO-Ir was also confirmed by several experiments.

Based on the above work, Lin and co-workers further developed three robust and porous bipyridyl- and phenanthryl-based metal–organic frameworks of UiO topology (BPV-MOF, mBPV-MOF, and mPT-MOF) (Scheme 9b) [43]. The post-synthetic metalation of these MOFs with $[Ir(COD)(OMe)]_2$ afforded three Ir-functionalized MOFs, which are highly active catalysts for the C–H borylation of a series of arenes and heteroarenes using B_2pin_2. Importantly, mBPV-MOF-Ir exhibited high TONs of up to 17,000 and could be recycled >15 times.

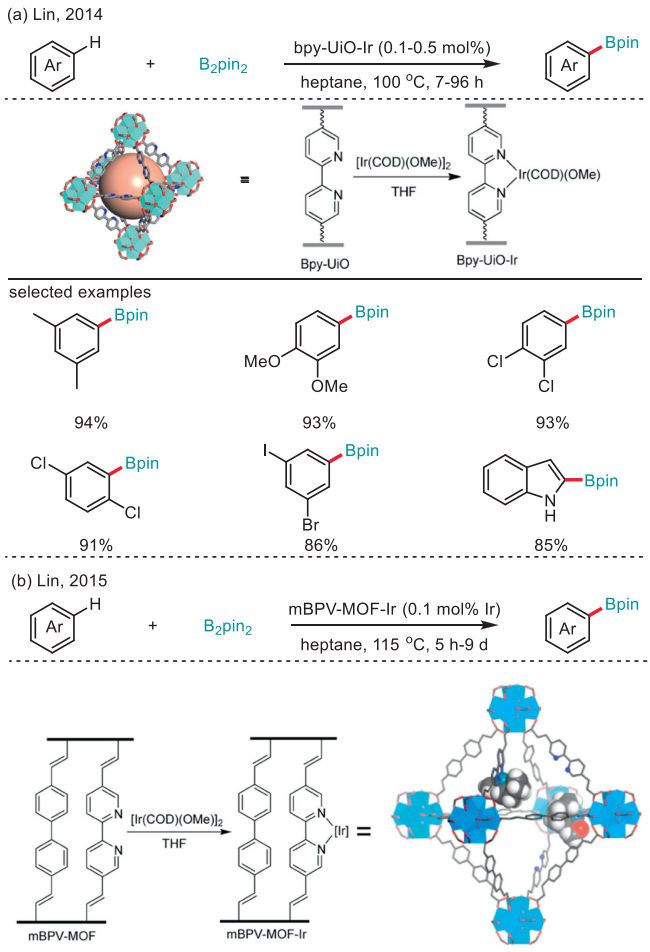

Scheme 9. bpy-UiO-Ir and mBPV-MOF-Ir-catalysed aromatic C–H borylation of arenes. Reproduced with permission [42]. Copyright 2014, American Chemical Society. Reproduced with permission [43]. Copyright 2015, American Chemical Society.

Besides the bipyridine ligand, the phosphine ligand could also be immobilized on the MOF support. In 2016, Lin and co-workers developed a porous triarylphosphine-based metal–organic framework, whose postsynthetic metalation with $[Ir(COD)(OMe)]_2$ afforded a MOFs-stabilized mono(phosphine)-Ir complexes (P1-MOF–Ir), which exhibited excellent catalytic activity for the C–H borylation of arenes (Scheme 10a) [44].

Three years later, Lin and co-workers employed a similar MOF-stabilized mono-phosphine-Ir catalyst (Zr-P1-Ir) as a highly active catalyst for methane borylation to afford the monoborylated product (Scheme 10b) [45]. Remarkably, Zr-P1-Ir significantly outperformed other Ir catalysts in methane borylation to exclusively afford CH_3Bpin with a TON of 127 at 110 °C. In addition, Zr-P1-Ir could be recovered as a crystalline solid from the methane borylation reaction mixture *via* centrifugation and reused in subsequent cycles of methane borylation with some decreases in B_2pin_2 conversions, CH_3Bpin yields, and TONs. Experimental and computational studies revealed that MOF stabilizes the homogeneously inaccessible, low-coordinate (P1)$Ir(Boryl)_3$ catalyst to provide a unique strategy to significantly lower the activation barrier of methane borylation. The reaction is proposed to begin with the

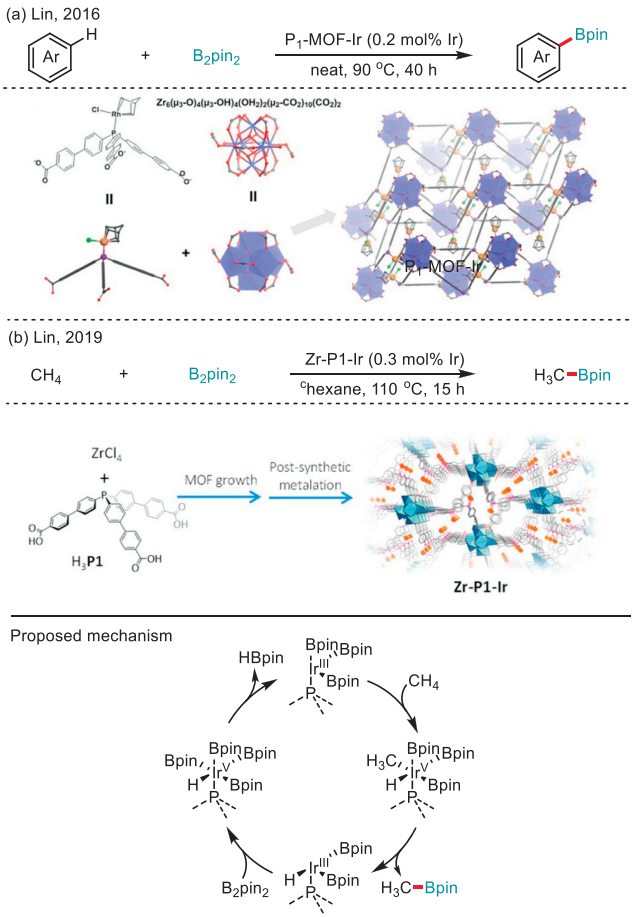

Scheme 10. P1-MOF-Ir-catalysed aromatic C–H borylation of arenes and Zr-P1-Ir-catalysed C–H borylation of methane. Reproduced with permission [44]. Copyright 2016, American Chemical Society. Reproduced with permission [45]. Copyright 2019, American Chemical Society.

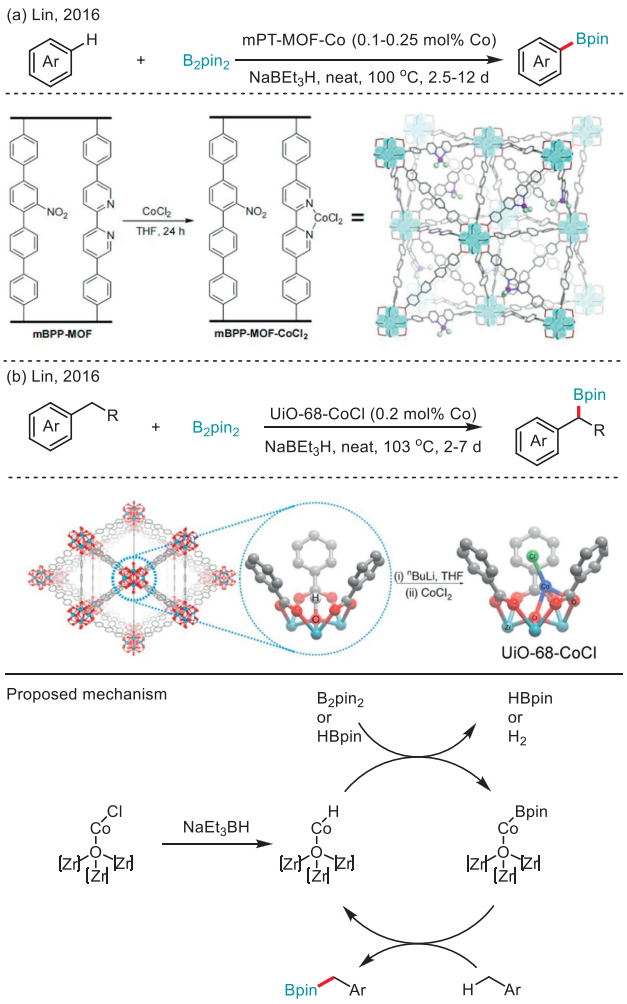

Scheme 11. mPT-MOF-Co-catalysed aromatic C–H borylation of arenes and UiO-68-CoCl-catalysed benzylic C–H borylation of alkylarenes. Reproduced with permission [46]. Copyright 2016, American Chemical Society. Reproduced with permission [47]. Copyright 2016, Springer Nature.

oxidative addition of (P1)Ir^{III}(boryl)$_3$, which cleaves the C–H bond of methane, forming a six-coordinate (P1)Ir^{V}(boryl)$_3$(CH_3)(H) intermediate. Reductive elimination of this Ir^{V} intermediate produces (P1)Ir^{III}(boryl)$_2$(H) and the CH_3Bpin product. The regeneration of the (P1)Ir^{III}(boryl)$_3$ catalyst involves another Ir^{III}/Ir^{V} oxidative addition and reductive elimination cycle, in which one B_2pin_2 is consumed and one HBpin is produced as a byproduct.

New and active earth-abundant metal catalysts are critically needed for sustainable chemical synthesis. Based on their previous works on heterogeneous MOF-Ir catalysis, Lin and co-workers further explored the cobalt-bipyridine- and cobalt-phenanthroline-based metal–organic framework catalysts for the arene C–H borylation (Scheme 11a) [46]. The same group also reported the preparation of a highly active and reusable single-site solid catalyst, UiO-68-CoCl, which showed high catalytic activities for the benzylic C–H borylation of alkylarenes (Scheme 11b) [47]. With a 1.0 mol% Co loading, the UiO–Co catalyst can be reused at least five times for the borylation of *p*-xylene. Based on experimental observations, the proposed mechanism begins with the reaction of the 'Zr_3-μ_4-O-Co-Cl' moiety in UiO–CoCl with $NaEt_3BH$, generating the active UiO–CoH species. A subsequent σ-bond metathesis between Co-H and B_2pin_2 forms Zr_3-μ_4-O-Co-Bpin species. This species then reacts with the alkylarene in a four-centered turnover-limiting step involving a $[2\sigma+2\sigma]$ cycloaddition of the 'Co–Bpin' bond with the 'H–CH_2Ar' bond of the alkylarene, producing benzyl boronates and regenerating UiO–CoH. Despite the electron-deficient Co catalyst favoring electron-rich aryl C–H bonds, the steric hindrance from the three phenyl rings around the Co center directs the selective binding to less-hindered benzylic C–H bonds.

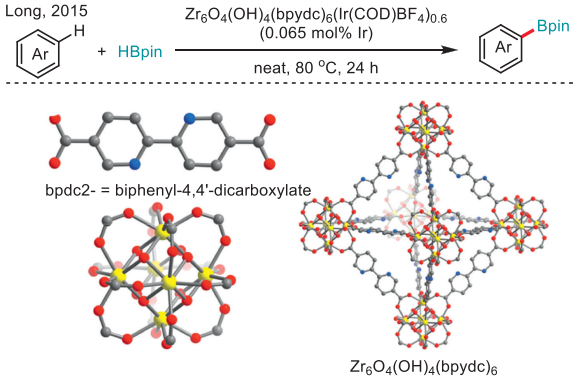

Scheme 12. $Zr_6O_4(OH)_4(bpydc)_6(Ir(COD)BF_4)_{0.6}$-catalysed C–H borylation of arenes. Reproduced with permission [48]. Copyright 2015, American Chemical Society.

In parallel with Lin's work, in 2015, Long and co-workers reported a similar work employing $Zr_6O_4(OH)_4(bpydc)_6(Ir(COD)BF_4)_{0.6}$ as the precatalyst for the C–H borylation of arenes using HBpin as the boron source under neat conditions (Scheme 12) [48]. Catalyst cycling experiments showed no significant loss in activity over five cycles.

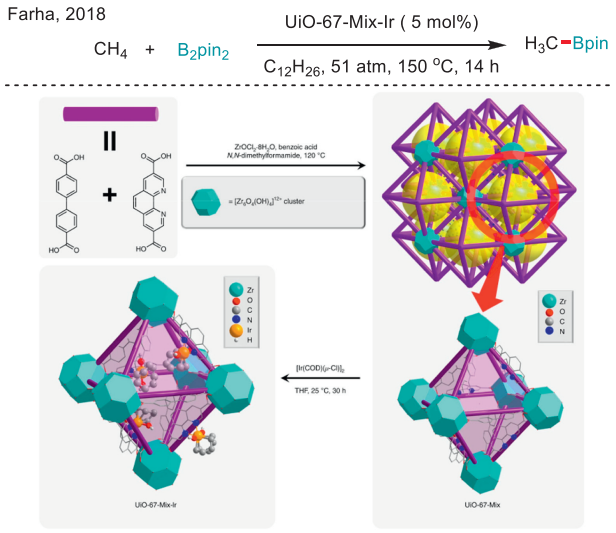

Scheme 13. UiO-67-Mix-Ir-catalyzed C–H borylation of methane. Reproduced with permission [49]. Copyright 2018, Springer Nature.

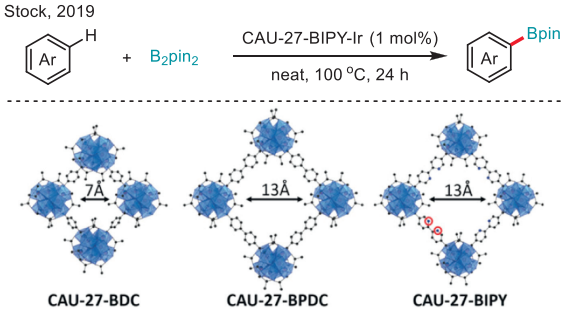

Carbon: black, Hydrogen: not displayed, Nitrogen atoms of CAU-27-BIPY are displayed in blue and highlighted by red circles, Zr-O IBU: blue.

Scheme 14. CAU-27-BIPY-Ir-catalysed C–H borylation of arenes. Reproduced with permission [51]. Copyright 2019, John Wiley and Sons.

By employing a mixed-linker 'doping' method, a UiO-67-like MOF, UiO-67-Mix, was prepared by Farha and co-workers in 2018 (Scheme 13) [49]. The subsequent metalation of UiO-67-Mix with $[Ir(COD)(\mu\text{-}Cl)]_2$ yielded initially a green inactive catalyst UiO-67-Mix-Ir-green, which was spontaneously oxidized in air to generate UiO-67-Mix-Ir, an orange microporous MOF-supported iridium(III) catalyst. UiO-67-Mix-Ir exhibited good catalytic activity in methane borylation to afford monoborylated methane CH_3Bpin in 19.5% yield (TON = 67) in dodecane, at 150 °C and 34 atm of methane. The high chemoselectivity for the monoborylation of methane is ascribed to the shape-selective effect of the microporous MOF pore structures. In 2020, a detailed mechanistic investigation on UiO-67-Mix-Ir-catalysed C–H borylation of arenes was reported by the same group [50].

During the investigation of green and sustainable solvents for the synthesis of Zr-MOFs, Stock and co-workers discovered two new crystalline compounds (CAU-26 and CAU-27-BDC) upon reacting terephthalic acid (H_2BDC) and zirconium acetate in pure acetic acid under solvothermal conditions (Scheme 14) [51]. Two isoreticular derivatives of CAU-27 (CAU-27-BPDC and CAU-27-BIPY) with extended linker molecules were also synthesized by implementing 4,4′-biphenyldicarboxylic acid (H_2BPDC) and 5,5′-dicarboxy-2,2′-bipyridine (H_2BIPY). CAU-27-BIPY was loaded with $[Ir(COD)(OMe)]_2$ through post-synthetic metalation to create CAU-27-BIPY-Ir, an efficient heterogeneous catalyst for the C–H borylation of arenes with various functional groups. Notably, CAU-27-BIPY-Ir demonstrates better recycling performance than the well-known UiO-67-BIPY-Ir. It has be reused twice in the borylation of toluene with a slight loss of catalytic activity in the second run and a significant loss in the third run.

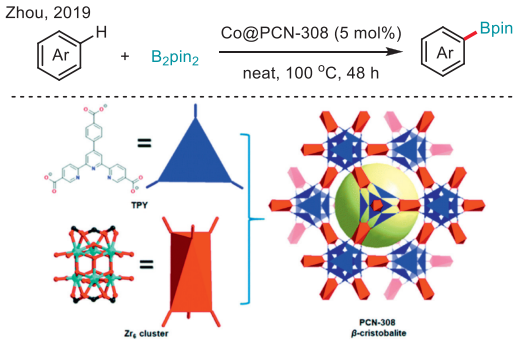

Scheme 15. Co@PCN-308-catalyzed C–H borylation of arenes. Reproduced with permission [52]. Copyright 2019, the Royal Society of Chemistry.

In 2019, Zhou and co-workers reported a Zr-based mesoporous MOF with predictable β-cristobalite topology, PCN-308, which was prepared by using a tritopic terpyridine-based linker (H_3TPY) (Scheme 15) [52]. The facile post-synthetic metalation of PCN-308 with $Co(OAc)_2$ afforded the scaffolded MOF material Co@PCN-308, which exhibits highly efficient catalytic activity for C–H borylation of arenes with B_2pin_2. The catalyst can also be reused for at least three cycles without significant loss of catalytic activity.

With the interest in developing robust base metal catalysts with Schiff base ligands, in 2020, Manna and co-workers reported a MOF-cobalt-catalyst, pyrim-MOF-Co, which was prepared by the metalation of pyridylimine-functionalized zirconium-MOF (pyrim-MOF) with $CoCl_2$ followed by treatment of $NaEt_3BH$ (Scheme 16a) [53]. Pyrim-MOF-Co was found to be an active catalyst for the aromatic C−H borylation of various arenes and heteroarenes using B_2pin_2 and benzylic C−H borylation of alkylarenes using HBpin. Impressively, pyrim-MOF-Co gave a TON of up to 2500 for the aromatic C–H borylation of *o*-xylene and could be recovered and reused at least 9 times without significant loss of catalytic activity. Based on spectroscopic, kinetic, and computational studies, a mechanism was proposed. Initially, B_2pin_2 undergoes oxidative addition to the cobalt center of (pyrim)Co(THF), forming (pyrim)Co(Bpin)$_2$. This species then undergoes a turnover-limiting σ-bond metathesis with the arene C−H bond, producing (pyrim)Co(H)(Bpin) and arylboronate. Following this, coordination of THF to the cobalt in (pyrim)Co(H)(Bpin) and subsequent reductive elimination regenerate the active state of the Co-catalyst, completing the catalytic cycle.

Two years later, a metal-organic framework supported mono-ligated phosphine-cobalt complex, MOF-P-Co, was developed by the same group as an active heterogeneous catalyst for aromatic C–H borylation (Scheme 16b) [54]. Importantly, this mono(phosphine)-Co catalyst gave a TON up to 30,000 and could be recovered and reused at least 13 times. Very recently, they reported the Pyrim-UiO-IrH MOF, a highly robust and effective heterogeneous catalyst for the C–H borylation of methane, yielding CH_3Bpin in nearly quantitative amounts with a TON of 196 (Scheme 16c) [55]. The Pyrim-UiO-Ir catalyst can be recycled and reused at least five times while maintaining consistent activity and showing no significant changes in structure or crystallinity.

By employing a dispersing-etching strategy, Li and co-workers successfully prepared A-Pt NB, an amorphous nanobox (NB) with high-density atomic platinum species by cation exchange with the ZIF-8 (ZIF = zeolitic imidazolate framework) precursor (Scheme 17a) [56]. The high-density atomic Pt nanoboxes exhibit excellent

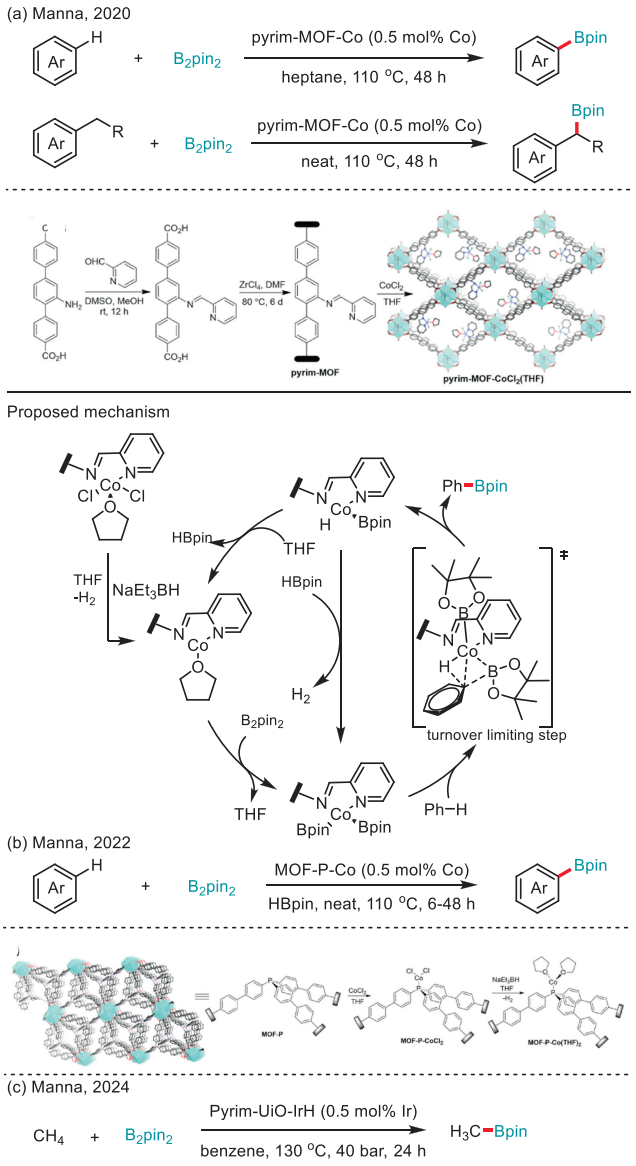

Scheme 16. Pyrim-MOF-Co-catalyzed aromatic C–H borylation of arenes and benzylic C–H borylation of alkylarenes, MOF-P-Co-catalyzed C–H borylation of arenes, and Pyrim-UiO-IrH-catalyzed C–H borylation of methane. Reproduced with permission [53]. Copyright 2020, American Chemical Society. Reproduced with permission [54]. Copyright 2022, John Wiley and Sons. Reproduced with permission [55]. Copyright 2024, the Royal Society of Chemistry.

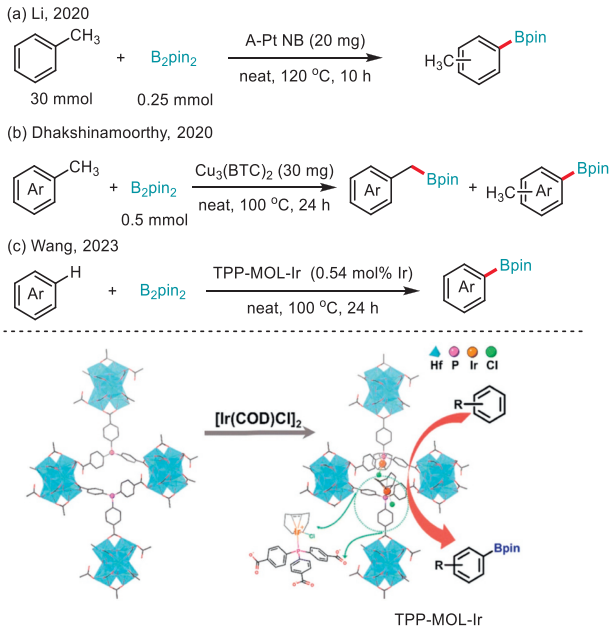

Scheme 17. A-Pt NB-catalyzed aromatic C–H borylation of toluene, $Cu_3(BTC)_2$-catalyzed benzylic and aromatic C–H borylation of arenes, and TPP-MOL-Ir-catalyzed C–H borylation of arenes. Reproduced with permission [58]. Copyright 2023, the Royal Society of Chemistry.

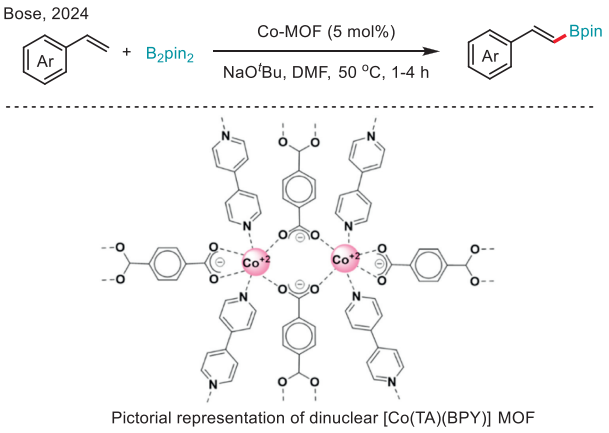

Scheme 18. Co-MOF-catalyzed C–H borylation of arenes. Reproduced with permission [59]. Copyright 2024, American Chemical Society.

performance for the C–H borylation of a diverse range of arenes with different substituents. The catalyst maintained its activity well after three cycles without requiring any additional reactivation. Dhakshinamoorthy and co-workers reported that the commercially available MOF $Cu_3(BTC)_2$ is an effective heterogeneous catalyst to promote benzylic and aromatic C–H borylation of arenes (Scheme 17b) [57]. The activity of $Cu_3(BTC)_2$ was retained over two reuses, with no changes in conversion rates or product distributions.

Recently, based on a Zr–phosphine oxide-based MOF (TPO-MOF), Wang and co-workers reported the synthesis of TPP-MOL, a phosphine-containing metal-organic layer (MOL) constructed from Hf_6-oxo secondary building units (SBUs) and tris(4-carboxylphenyl)phosphine (TPP) ligands (Scheme 17c) [58]. The metalation of TPP-MOL with $[Ir(COD)Cl]_2$ produced TPP-MOL-Ir, a highly effective heterogeneous catalyst for the C–H borylation of arenes, including sterically demanding ones that are challenging for 3D MOF catalysts. TPP-MOL-Ir can be reused three times for the borylation of chlorobenzene without any loss of catalytic activity. However, its activity decreases significantly after the fourth use.

Selective direct dehydrogenative borylation of alkenes is a valuable method for synthesizing vinyl boronic esters. Very recently, Bose and co-workers reported a dehydrogenative borylation of terminal alkenes using a cobalt-metal-organic framework (Co-MOF) as the catalyst and dimethylformamide as a hydrogen scavenger (Scheme 18) [59]. Notably, the catalyst could be reused up to five times with no significant loss in activity.

2.4. COFs-supported metal catalysts and COFs-based photocatalyst

Owing to their tunable compositions, structures, functions, and porosity, covalent organic frameworks (COFs) have emerged as robust materials for various applications, especially catalysis. In 2018, Cui and co-workers prepared a series of two-, three-, and four-component 2D COFs with AA, AB, or ABC stacking

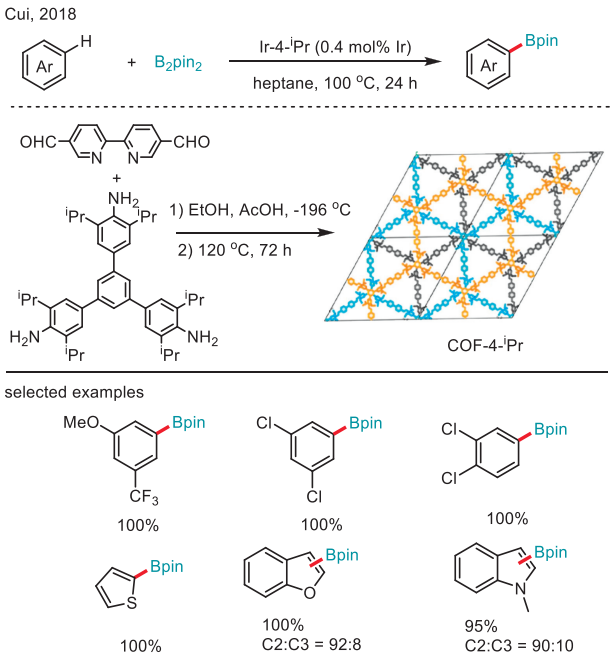

Scheme 19. Ir-4-^{i}Pr-catalyzed C–H borylation of arenes. Reproduced with permission [60]. Copyright 2018, American Chemical Society.

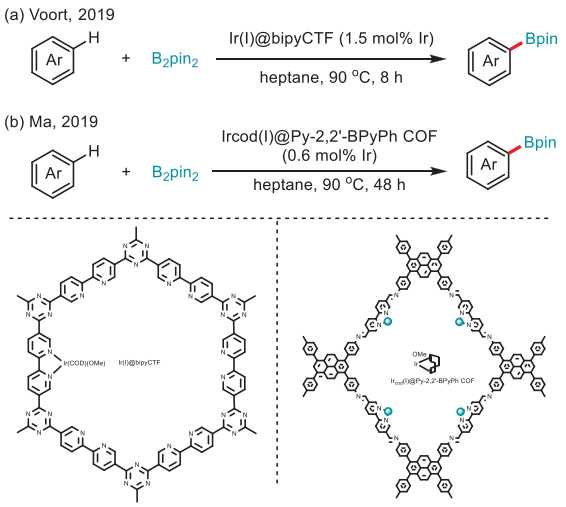

Scheme 20. Ir(I)@bipyCTF- and Ircod(I)@Py-2,2′-BPyPh COF-catalyzed C–H borylation of arenes.

by co-condensation of triamines with and without alkyl substituents (ethyl and isopropyl) and di- or trialdehyde building blocks (Scheme 19) [60]. The layer stacking and chemical stability of these 2D COFs were controlled by managing interlayer steric hindrance *via* a multivariate (MTV) approach. The post-synthetic metalation of three 2,2′-bipyridyl-derived COFs (4-^{i}Pr, 4-Et, 4-H) with $[Ir(COD)(OMe)]_2$ gave three Ir-COFs, Ir-4-^{i}Pr, Ir-4-Et and Ir-4-H, which were active catalysts for the C−H borylation of arenes and heteroarenes. Owing to its increased porosity and chemical stability, Ir-4-^{i}Pr exhibits much higher catalytic activity than Ir-4-Et and Ir-4-H. Notably, Ir-4-^{i}Pr can be reused at least ten times in the borylation of 3-(trifluoromethyl)anisole without loss of catalytic activity.

In 2019, Voort and co-workers reported a heterogeneous arene borylation catalyst prepared by the post-metalation of a bipyridine-based metal-modified covalent triazine framework (bipyCTF) with $[Ir(OMe)(cod)]_2$, which could be reused for at least five cycles without significant loss of activity (Scheme 20a) [61]. In the same year, Ma and co-workers prepared an iridium-immobilized framework catalyst *via* the immobilization of catalytically active iridium ions on a two-dimensional covalent organic framework with bipyridine moieties using a programmed synthetic procedure (Scheme 20b) [62]. This catalyst exhibits excellent activity for the C–H borylation of arenes and can be reused for up to four catalytic cycles while maintaining its activity.

Recently, based on Leonori's work [63], Banerjee and co-workers reported the visible-light-driven metal-free C−H borylation of azines with $Me_3N{-}BH_3$ using highly stable β-ketoenamine-based COFs as polymeric pigment photocatalysts (Scheme 21) [64]. Three different COFs TpAzo, TpDpp, and TpTab were synthesized following the solvothermal approach previously reported, in which TpAzo COF exhibits the highest catalytic activity because of its highest surface area, broader absorbance, and low band gap. The yields of the products are maximized near the COF's absorption maxima indicating that the light absorbance capacity of the COF plays a critical role during catalysis. Keto-enamine tautomerization imparts the desired stability to the COF backbone during catalysis, barring it from photo- and chemical decomposition. Therefore, TpAzo COF could be easily recovered from the reaction mixture by centrifugation and reused as the solid photocatalyst for the same reaction for five cycles. A similar mechanism to that of the homogeneous counterpart has been proposed. In this mechanism, the one-electron reduction of ammonium persulfate by COFs in an excited state generates sulfate radicals. These radicals then abstract a hydrogen atom from trimethylamine–borane, producing a boryl radical. This boryl radical couples with the protonated azine ring *via* a "Minisci addition" to form a radical cation, **A**. The radical cation then undergoes rearomatization to produce the final product, **B**, through one of two pathways: (i) one-electron oxidation by the photogenerated hole of the COF followed by proton elimination, or (ii) one-electron oxidation by the persulfate followed by proton elimination.

2.5. Organic polymer-supported FLP and metal catalysts

To generate heterogeneous supported frustrated Lewis pair (FLP) catalysts for the C–H borylation of heteroarenes [65,66], in 2019, Fontaine and co-workers prepared P-Me, P-Et, and P-Pip, three polymeric versions of previously developed *ansa-N,N*-dialkylammoniumtrifluoroborate ambiphilic molecules based on the styrene motif (Scheme 22a) [67]. These heterogeneous precatalysts could enable the C–H borylation of electron-rich heteroarenes although their activity is lower than the homogeneous analogues. Moreover, polymer P-Et proved durable conserving the same catalytic activity after three runs.

Recently, two porous organic polymers (POPs) based on polystyrene-bearing bipyridine ligands, bpy-PS-POP and bpy-^{t}BuPS-POP, were synthesized by Kegnæs and co-workers (Scheme 22b) [68]. The metal ligation of the POPs with $[Ir(cod)Cl]_2$ created active catalysts enabling the C–H borylation of arenes. The system was recyclable for up to three consecutive recycles, albeit the activity was lost upon further usage.

2.6. Metal oxide- and zeolite-supported metal catalysts

With reference to the previously reported homogeneous copper-carbenes-catalyzed dehydrogenative borylation of styrenes [69], in 2019, Yamaguchi and co-workers reported a heterogeneous copper-catalyzed dehydrogenative borylation of styrene derivatives with B_2pin_2 under ligand- and base-free conditions (Scheme 23a) [70]. Various β-monoborylstyrenes were obtained by using

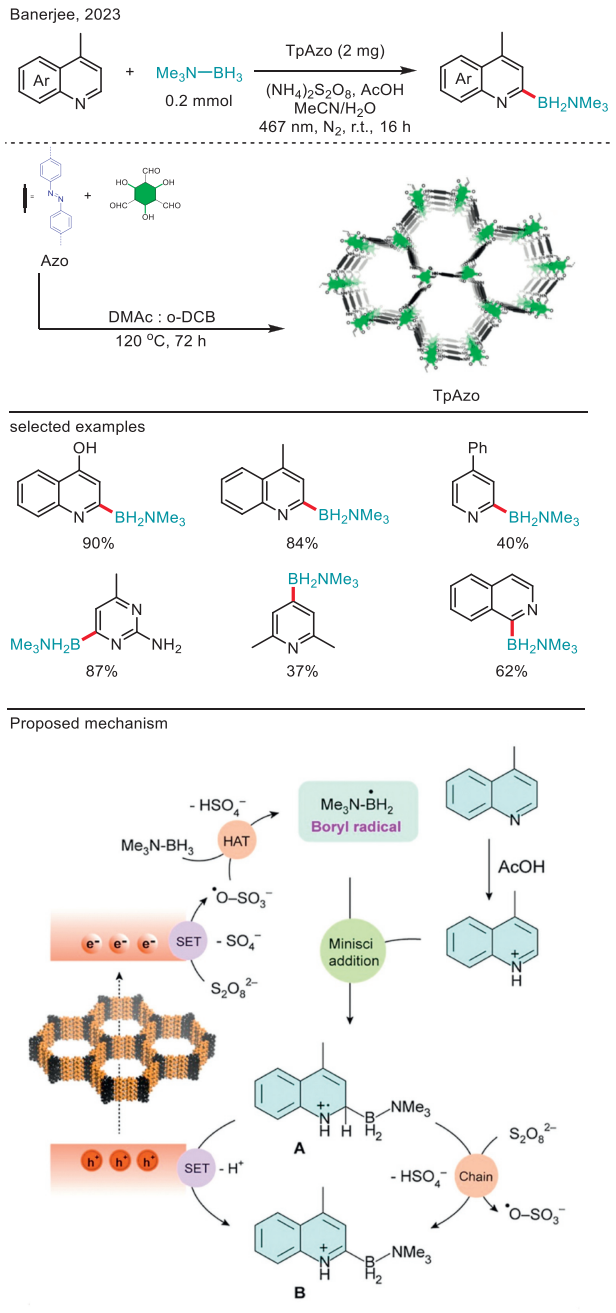

Scheme 21. Visible-light-driven TpAzo-catalyzed C–H borylation of azines. Reproduced with permission [64]. Copyright 2023, American Chemical Society.

$Cu(OH)_x/CeO_2$ as the catalyst and benzophenone as HBpin acceptor, while the combination of $Cu(OH)_x/Al_2O_3$ and 2-adamantanone with increased amount of B_2pin_2 afforded β,β-diborylstyrenes. The catalysts could be reused several times, though their catalytic performance gradually declined. By using a highly dispersed Ni hydroxide species supported on CeO_2 as the catalyst, the same group achieved the benzylic C–H borylation of alkylarenes using HBpin as the borylating agent (Scheme 23b) [71]. The reusability of $Ni(OH)_x/CeO_2$ was also tested, but a significant loss of catalytic activity was observed during the reuse experiments.

In 2022, Qi and co-workers reported a zeolite-supported lanthanide $La(BH_4)_x$-HY_{30} catalyzed C–H borylation of benzene with HBpin (Scheme 24) [72]. A turnover number of 167 is accessed by capping external silanols, selectively grafting at BAS sites, and adding HBpin slowly to the reaction.

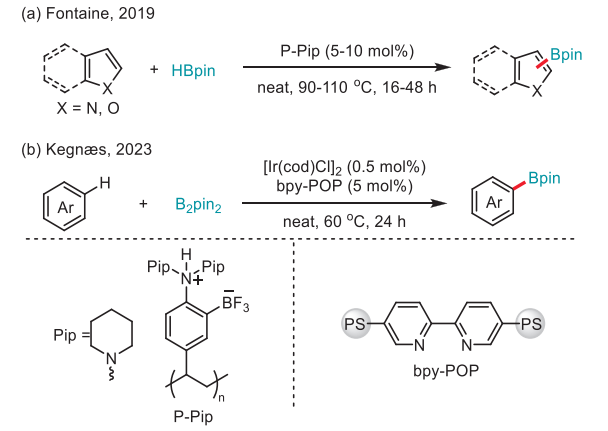

Scheme 22. P-Pip-catalyzed C–H borylation of heteroarenes and Ir/bpy-PS-POP-catalyzed C–H borylation of arenes.

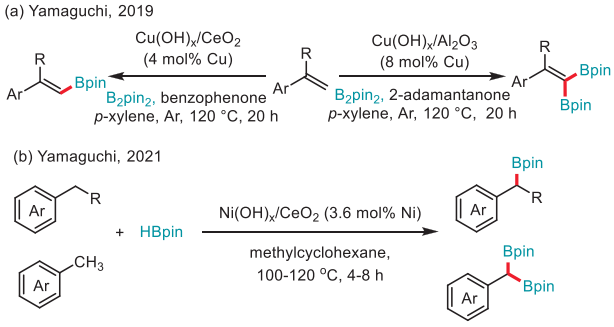

Scheme 23. $Cu(OH)_x/CeO_2$- and $Cu(OH)_x/Al_2O_3$-catalysed dehydrogenative borylation of styrene derivatives and $Ni(OH)_x/CeO_2$-catalysed benzylic C–H borylation of alkylarenes.

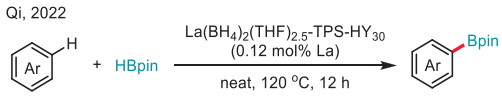

Scheme 24. $La(BH_4)_2(THF)_{2.5}$-TPS-HY_{30}-catalysed C–H borylation of benzene.

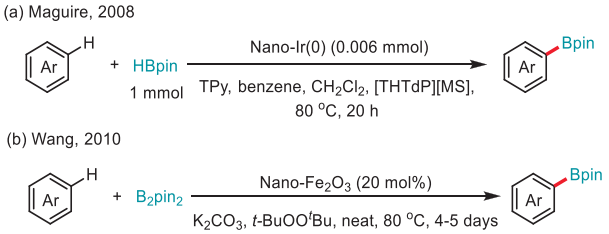

Scheme 25. Nano-Ir(0)- and Nano-Fe_2O_3-catalysed C–H borylation of arenes.

2.7. Others

Owing to their high surface areas and high density of active sites, nanoscale metal particles have been widely explored as catalysts [73]. In 2008, Maguire and co-workers prepared well-dispersed iridium(0) nanoparticles stabilized by the ionic liquid *via* the reduction of a hydridoiridium carborane precursor (Scheme 25a) [74]. The obtained iridium nanoparticles were found to be active catalysts for the C–H borylation of arenes and could be reused >6 times with essentially no loss in activity.

In 2010, Wang and co-workers reported a γ-Fe_2O_3 nanoparticles-catalyzed aromatic C–H borylation of arenes using B_2pin_2 as the borylating reagent under neat conditions (Scheme 25b) [75]. Impressively, the regioselectivity in this reac-

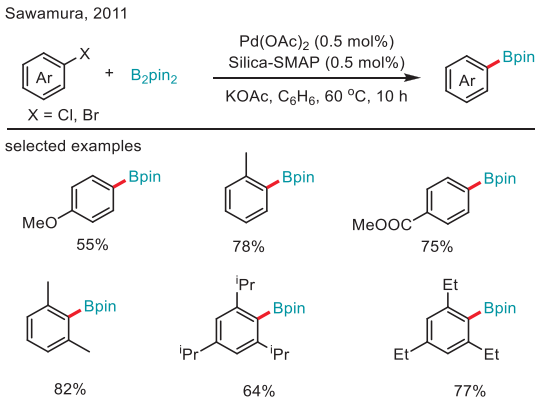

Scheme 26. Silica-SMAP/Pd-catalyzed C–X borylation of aryl halides.

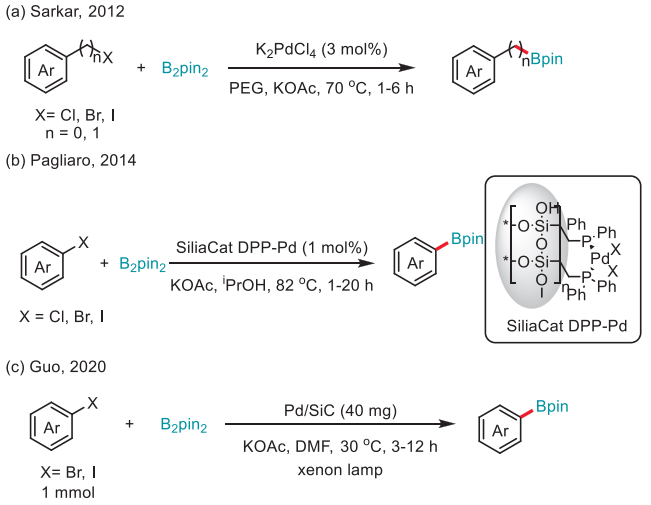

Scheme 27. Heterogeneous Pd-catalyzed C–X borylation of aryl and benzylic halides.

tion is controlled by the electronic effect of the substituents but not the steric effect, which is different from homogeneous Ir- and Rh-catalysis.

3. Heterogeneous C–X borylation

Over the past three decades, Miyaura borylation has rapidly advanced since its first report in 1995 [6]. Initially, the electrophiles used in Miyaura borylation were limited to organic halides (I, Br, and Cl). However, the range has since expanded to include substrates with various C–Het bonds (C–F, C–O, C–S, C–N) [9,11]. Recent progress in heterogeneous C–X borylation has introduced new methods for the efficient synthesis of organoboron compounds, including C–Halo borylation of aryl, alkyl, and benzyl halides (I, Br, Cl) and C–O borylation of alkyl, allyl, and benzyl acetates, as well as propargyl carbonates.

3.1. Pd catalysts

By employing their previously developed Silica-SMAP, in 2011, Sawamura and co-workers reported a heterogeneous Silica-SMAP/Pd-catalyzed borylation of aryl chlorides and bromides with B_2pin_2 (Scheme 26) [76]. Remarkably, sterically and electronically challenging aryl halides were suitable substrates in this borylation reaction. This silica-SMAP/Pd catalytic system is comparable to or exceeds that of homogeneous palladium systems with biphenyl-based "bulky" phosphane ligands such as XPhos and SPhos in the borylation of moderately challenging substrates such as 2,6-dimethylchlorobenzene. The borylation of several sterically extremely challenging substrates including 2,4,6-triethyl- and 2,4,6-triisopropylchlorobenzenes was achieved for the first time. Unfortunately, attempts to reuse the catalysts were unsuccessful.

In the following year, Sarkar and co-workers reported that palladium nanoparticles generated in PEG could catalyze the borylation of aryl and benzyl halides with B_2pin_2 under solvent-free and ligand-less conditions (Scheme 27a) [77]. Recycling experiments showed a decrease in yield, from 72% in the first cycle to 40% in the fifth cycle, indicating a deterioration of the catalyst.

In 2014, Pagliaro and co-workers reported a sol-gel entrapped SiliaCat diphenylphosphine palladium (SilicaCat DPP-Pd) catalyzed borylation of aryl chlorides, bromides, and iodides with B_2pin_2 (Scheme 27b) [78]. A wide range of functional groups were tolerated with very low (<5 ppm) leaching of valued Pd during catalysis. This transformation can also be conducted underflow, allowing the fast and clean borylation of aryl halides [79]. This catalyst decomposes upon reuse, although it generally performs effectively for up to four catalytic cycles, producing the desired product in nearly quantitative yield each time.

By employing a hierarchical SiC nanowire-supported Pd nanoparticles catalyst, in 2020, Guo and co-workers achieved the borylation of aryl bromides and iodides with B_2pin_2 under visible light irradiation and mild conditions (Scheme 27c) [80]. The SiC/Pd Mott-Schottky contact enhances the rapid transfer of the photogenerated electrons from SiC to the Pd nanoparticles resulting in concentrated energetic electrons in the Pd nanoparticles, which can facilitate the cleavage of C–Halo bonds. Importantly, the Pd/SiC catalyst could be recovered and reused for five cycles with no measurable loss in catalytic activity.

3.2. Cu catalysts

Copper-based catalysts are quite attractive in C–X borylation due to their low toxicity, low environmental impact, high abundance, and low cost. In 2014, Chung and co-workers reported the borylation of primary and secondary alkyl bromides with B_2pin_2 employing commercially available copper nanoparticles (Cu NPs) as the catalyst under ligand-free and room-temperature conditions (Scheme 28a) [81]. The observation of the ring-opening product in the reaction of cyclopropylmethyl bromide supported a radical-involved pathway. One year later, Xu and co-workers reported a carbon black (CB) supported Cu_2O nanoparticles (Cu_2O NPs/CB) catalyzed borylation of primary and secondary alkyl bromides using B_2pin_2 or $B_2(neop)_2$ under mild and ligand-free reaction conditions (Scheme 28b) [82]. Notably, this catalyst could be recovered from the reaction mixture by centrifugation and reused for three cycles with only a slight decrease in catalytic activity.

By using a magnetically separable dopamine (DOPA) functionalized nano-ferrite-supported Cu nanoparticles (Fe-DOPA-Cu NPs) catalyst, in 2020, Bose and co-workers achieved the borylation of alkyl chlorides, bromides, and iodides with B_2pin_2 under mild reaction conditions (Scheme 28c) [83]. Three years later, the same group reported the borylation of alkyl and aryl halides with B_2pin_2 by employing nitrogen-doped carbon nanotubes (N–CNT) supported copper nanoparticles (Cu/N–CNT) and carbon nanotubes (CNT) supported copper nanoparticles (Cu/CNT) respectively (Scheme 28d) [84]. Radical clock experiments revealed that both reactions proceeded *via* a radical-mediated process. Importantly, no significant loss of activity was observed after ten runs of catalyst recycling for both Fe-DOPA-Cu NPs and Cu/N–CNT catalysts.

In 2021, Cid and co-workers reported the borylation of both aliphatic and aromatic halides with B_2pin_2 catalyzed by graphite nanoplatelets (GNP) supported Cu(I) materials (Scheme 28e) [85].

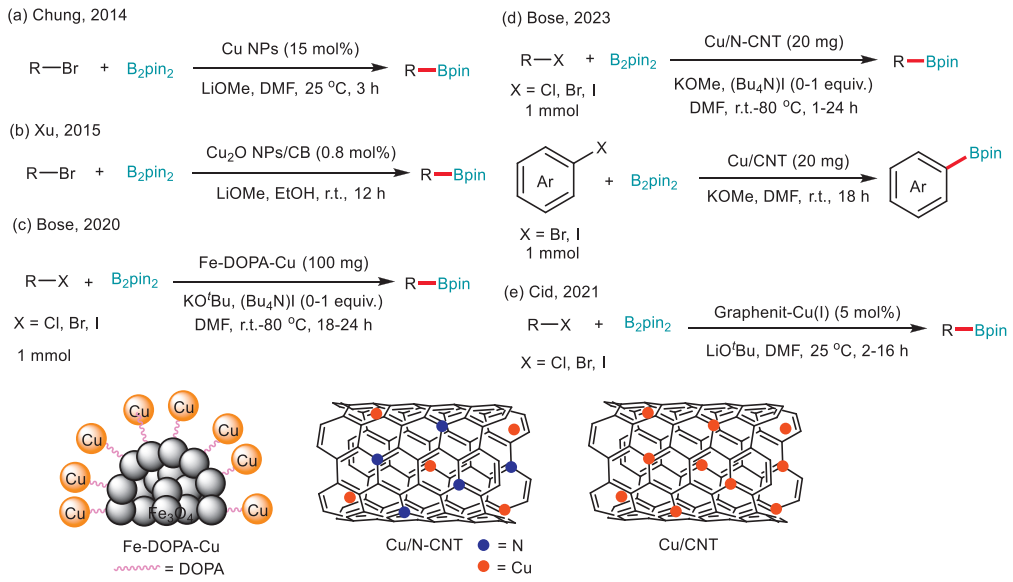

Scheme 28. Heterogeneous Cu-catalyzed C–X borylation of aryl and alkyl halides.

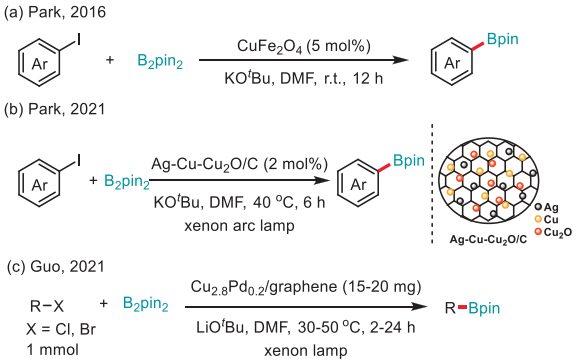

Scheme 29. Heterogeneous bimetallic catalysts-catalyzed C–X borylation of aryl and alkyl halides.

These materials are easily recyclable for at least four cycles, and the reactions are scalable. An interesting synergetic performance of Cu_2O when anchored to a graphenic support was revealed by a detailed study of all the possible catalytic species and DFT calculations.

3.3. Bimetallic catalysts

By using commercially available, superparamagnetic copper ferrite nanoparticles, in 2016, Park and co-workers reported the borylation of aryl iodides and β-bromostyrenes with B_2pin_2 under ligand-free conditions (Scheme 29a) [86]. Five years later, the same group prepared a mixed metal–metal oxide/C (Ag–Cu–Cu_2O/C) nanocomposites by the heat treatment of a metal-organic framework Cu-BTC under a N_2 flow using the one-pot synthesis method (Scheme 29b) [87]. This Ag–Cu–Cu_2O/C catalyst showed high photocatalytic activity towards the borylation of aryl iodides under a xenon arc lamp and could be recycled seven times without any significant decrease in product yield or change in particle size.

In 2021, Guo and co-workers reported a graphene-supported Cu/Pd alloy nanoparticles ($Cu_{2.8}Pd_{0.2}$/graphene) catalyzed photocatalytic borylation of primary and secondary alkyl bromides and chlorides with B_2pin_2 or $B_2(neop)_2$ with visible light in the air (Scheme 29c) [88]. The synergistic effect of localized surface plasmon resonance (LSPR) of Cu and charge transfer from Cu to Pd due to the alloy surface charge heterogeneity of the Cu-Pd alloy nanoparticles surface is critical for the high performance of this heterogeneous catalyst. Notably, the $Cu_{2.8}Pd_{0.2}$/graphene catalyst could be recovered and reused for five cycles with no measurable loss in catalytic activity.

3.4. Metal oxide-supported Au catalyst

Transition-metal-catalyzed borylation of $C(sp^3)$–X bonds is one of the most promising methods for preparing important allyl, benzyl, and allenylboron compounds, in which major efforts have been devoted to homogeneous catalysis with only one heterogeneous example reported by Morken and co-workers on Pd/C-catalyzed borylation of allyl chloride [89]. In 2021, Shishido and co-workers reported an Au/TiO_2 (Au nanoparticles supported on TiO_2) catalyzed C–O borylation of allyl and benzyl acetates, and propargyl carbonates giving the corresponding allyl, benzyl, and allenyl boronic esters in high yields under mild phosphine- and base-free conditions (Scheme 30a) [90]. Remarkably, allylic and benzylic alcohols were also suitable substrates. This Au/TiO_2 catalyst exhibited high reusability, and no significant decreases in product yields were confirmed in four consecutive catalytic runs for both allyl and allenyl boronate synthesis. Based on a Hammett study and control experiments, an S_N1'-type mechanism has been proposed. Initially, diboron adsorbs onto the surface of gold nanoparticles (Au NPs), where the interaction between the oxygen atom of the boronate and the Lewis-acidic Au NPs enhances the Lewis acidity of the boron atom. Next, the ester and alkene groups in allyl esters coordinate with the boronate and the Au surface, respectively. This coordination triggers the cleavage of the C – O bond, generating an allyl cation and simultaneously forming a tetra-coordinated borate. The diborane-base adducts then release a nucleophilic boryl species. This activated boron species adds to the alkene moiety, and subsequent bond isomerization results in the formation of allyl boronates.

Very recently, building on their previous work [91,92], Shishido and co-workers advanced the C–O borylation of unactivated alkyl acetates using a supported Au catalyst (Au/ZrO_2) (Scheme 30b) [93]. The success of this transformation is attributed to the generation of alkyl radicals from alkyl acetates in the presence of the supported Au catalyst and disilane. Remarkably, the Au/ZrO_2 cata-

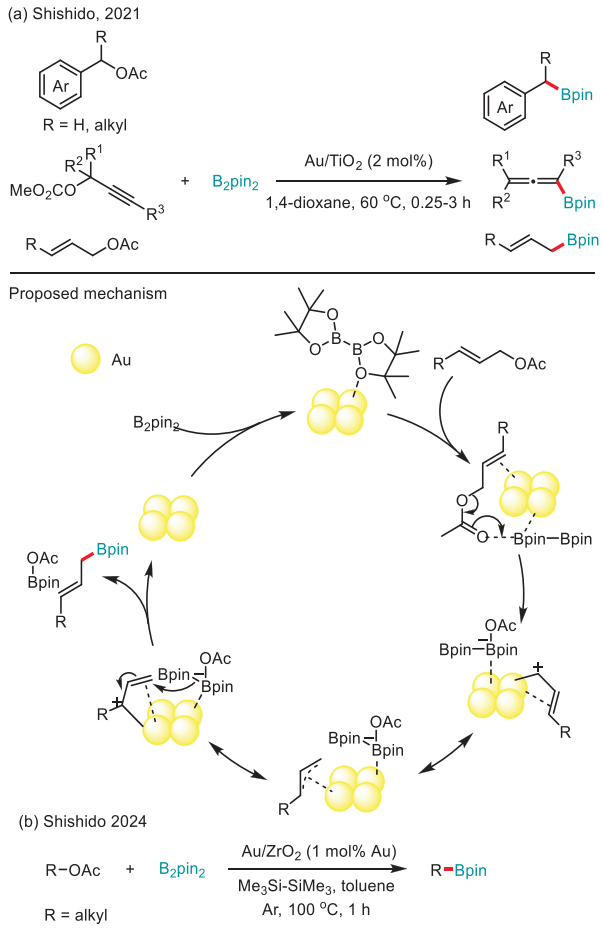

Scheme 30. Au/TiO_2-catalyzed C–O borylation of allyl and benzyl acetates, and propargyl carbonates, and Au/ZrO_2-catalyzed C–O borylation of unactivated alkyl acetates.

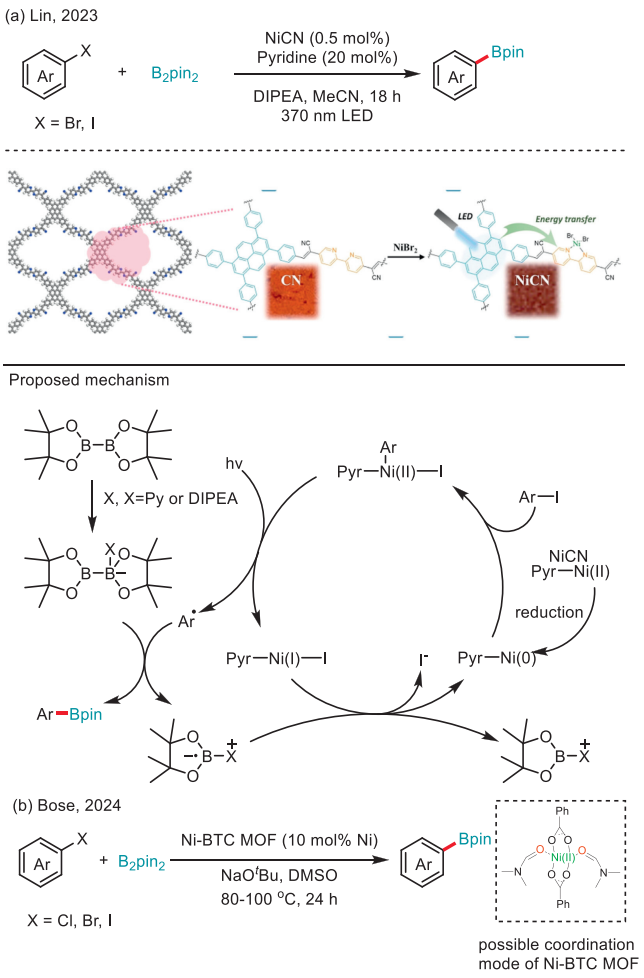

Scheme 31. Photoinduced NiCN-catalyzed, and Ni-BTC MOF-catalyzed C–X borylation of aryl halides. Reproduced with permission [94]. Copyright 2023, John Wiley and Sons.

lyst demonstrated excellent reusability for the borylation of alkyl acetates, maintaining product yield over four consecutive catalytic runs with no significant decrease.

3.5. Ni catalysts

In 2023, Lin and co-workers reported a COF-based energy transfer Ni catalysis for the C–X borylation of aryl iodides and bromides (Scheme 31a) [94]. They synthesized a pyrene-based COF with sp^2 carbon conjugation, which coordinated Ni^{II} centers *via* bipyridine moieties to form the NiCN catalyst. Remarkably, NiCN exhibited two orders of magnitude higher efficiency compared to its homogeneous counterpart and could be recovered and reused at least three times with minimal loss of catalytic activity. The proposed mechanism involves an energy transfer process: Ni^{II} is first photoreduced by pyrenes in NiCN using diisopropylethylamine (DIPEA) as a reductant. The resulting Ni^0-bipyridine complex undergoes oxidative addition with an aryl halide to form a Ni^{II}-aryl complex. Upon photoexcitation, the pyrene transfers energy to the Ni^{II}-aryl complex, facilitating the cleavage of the Ni–C bond and generating an aryl radical. This radical is captured by B_2pin_2 to produce the borylation product, while the remaining B_2pin_2 leaves as a boron radical anion, which reduces Ni^I to Ni^0, completing the catalytic cycle.

Very recently, Bose and co-workers developed a C–X borylation method using a nickel-benzene tricarboxylic acid metal–organic framework (Ni-BTC MOF) as the heterogeneous catalyst (Scheme 31b) [95]. This approach demonstrates broad functional group tolerance, and the catalyst can be recycled up to four times.

3.6. COF photocatalyst

In 2023, Chen and co-workers reported the photocatalytic borylation of aryl iodides with B_2pin_2 employing pyrene-based, nitrogen-rich, and imine-linked 2D COFs (N–COFs) as the photocatalyst under visible light irradiation (Scheme 32) [96]. Among the three N–COFs they prepared, 6N–COF exhibits excellent photocatalytic efficiency and superior recyclability, which could be attributed to its proper energy levels, broader light absorption, and high specific surface area. Notably, 6N–COF could be reused at least 10 times while preserving its catalytic activity.

4. Conclusion and outlook

In summary, the synthesis of organoboron compounds *via* heterogeneous C–H and C–X borylation has gained significant development in recent years. Aromatic, benzylic, and methane C–H borylation employing heterogeneous catalysts based on various supports such as carbon material, silica, MOFs/COFs material, metal oxide, zeolite, organic polymer, and so on have been developed for the efficient synthesis of organoboron compounds. Meanwhile, diverse aryl, alkyl, allyl, benzyl, and propargyl electrophiles have been converted to the corresponding organoboron compounds by

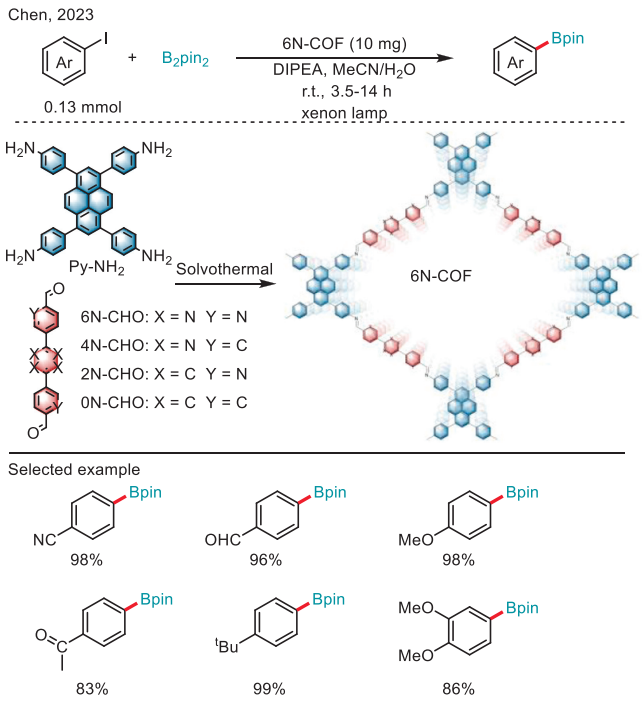

Scheme 32. Visible-light-driven 6N–COF-catalysed C–X borylation of aryl iodides.

C–X borylation employing various heterogeneous catalysts. Most of these heterogeneous catalysts show high activities in C–H and C–X borylation with good recycling properties. Although remarkable progress has been achieved, further research such as heterogeneous C–H borylation based on non-noble metals, heterogeneous site-selective C–H borylation of aliphatic C–H bonds besides benzylic C–H bonds and methane, heterogeneous C–X borylation of alcohols, phenols, ethers and amines, the comprehensive understanding of the original relationship between structural and the chemo- and regioselectivity and so on is still expected in this merging area. We believe that the continuous development of heterogeneous transformations will provide more practical and efficient methods for the preparation of organoboron compounds [28].

Declaration of competing interest

The authors declare that they have no known competing financial interests or personal relationships that could have appeared to influence the work reported in this paper.

CRediT authorship contribution statement

Shuai Tang: Writing – review & editing, Writing – original draft. **Zian Wang:** Writing – review & editing, Writing – original draft. **Mengyi Zhu:** Writing – review & editing, Writing – original draft. **Xinyun Zhao:** Writing – review & editing, Writing – original draft. **Xiaoyun Hu:** Writing – review & editing, Writing – original draft. **Hua Zhang:** Writing – review & editing, Writing – original draft.

Acknowledgments

This work was supported by grants from the National Natural Science Foundation of China (Nos. 22271313, 21602096), the Fund for Academic Innovation Teams of South-Central Minzu University (No. XTZ24015), and South-Central Minzu University.

References

[1] D. Hall, Boronic Acids: Preparation and Applications, Wiley, Weinheim, 2011.
[2] D.B. Diaz, A.K. Yudin, Nat. Chem. 9 (2017) 731–742.
[3] L. Ji, S. Griesbeck, T.B. Marder, Chem. Sci. 8 (2017) 846–863.
[4] S.K. Mellerup, S. Wang, Chem. Soc. Rev. 48 (2019) 3537–3549.
[5] G.F.S. Fernandes, W.A. Denny, J.L. Dos Santos, Eur. J. Med. Chem. 179 (2019) 791–804.
[6] T. Ishiyama, M. Murata, N. Miyaura, J. Org. Chem. 60 (1995) 7508–7510.
[7] M. Murata, S. Watanabe, Y. Masuda, J. Org. Chem. 62 (1997) 6458–6459.
[8] W.K. Chow, O.Y. Yuen, P.Y. Choy, et al., RSC Adv 3 (2013) 12518–12539.
[9] M. Wang, Z. Shi, Chem. Rev. 120 (2020) 7348–7398.
[10] L. Rout, T. Punniyamurthy, Coord. Chem. Rev. 431 (2021) 213675.
[11] Y.M. Tian, X.N. Guo, H. Braunschweig, U. Radius, T.B. Marder, Chem. Rev. 121 (2021) 3561–3597.
[12] P. Nguyen, H.P. Blom, S.A. Westcott, N.J. Taylor, T.B. Marder, J. Am. Chem. Soc. 115 (1993) 9329–9330.
[13] K.M. Waltz, X. He, C. Muhoro, J.F. Hartwig, J. Am. Chem. Soc. 117 (1995) 11357–11358.
[14] I.A.I. Mkhalid, J.H. Barnard, T.B. Marder, J.M. Murphy, J.F. Hartwig, Chem. Rev. 110 (2010) 890–931.
[15] A. Ros, R. Fernandez, J.M. Lassaletta, Chem. Soc. Rev. 43 (2014) 3229–3243.
[16] L. Xu, G. Wang, S. Zhang, et al., Tetrahedron 73 (2017) 7123–7157.
[17] J.S. Wright, P.J.H. Scott, P.G. Steel, Angew. Chem. Int. Ed. 60 (2021) 2796–2821.
[18] B. Su, J.F. Hartwig, Angew. Chem. Int. Ed. 61 (2022) e202113343.
[19] R. Bisht, C. Haldar, M.M.M. Hassan, et al., Chem. Soc. Rev. 51 (2022) 5042–5100.
[20] I.F. Yu, J.W. Wilson, J.F. Hartwig, Chem. Rev. 123 (2023) 11619–11663.
[21] H. Yang, Z. Zhou, C. Tang, F. Chen, Chin. Chem. Lett. 35 (2024) 109257.
[22] T. Ishiyama, K. Ishida, J. Takagi, N. Miyaura, Chem. Lett. (2001) 1082–1083.
[23] K. Maeda, K. Motokura, Synthesis 53 (2021) 3227–3234.
[24] S. Kawamorita, H. Ohmiya, K. Hara, A. Fukuoka, M. Sawamura, J. Am. Chem. Soc. 131 (2009) 5058–5059.
[25] S. Kawamorita, R. Murakami, T. Iwai, M. Sawamura, J. Am. Chem. Soc. 135 (2013) 2947–2950.
[26] R. Murakami, K. Tsunoda, T. Iwai, M. Sawamura, Chem. Eur. J. 20 (2014) 13127–13131.
[27] S. Konishi, S. Kawamorita, T. Iwai, et al., Chem. Asian J. 9 (2014) 434–438.
[28] H.H. Al Mamari, J. Borel, A. Hickey, et al., Chem. Eur. J. 29 (2023) e202301734.
[29] S. Kawamorita, T. Miyazaki, H. Ohmiya, T. Iwai, M. Sawamura, J. Am. Chem. Soc. 133 (2011) 19310–19313.
[30] S. Kawamorita, T. Miyazaki, T. Iwai, H. Ohmiya, M. Sawamura, J. Am. Chem. Soc. 134 (2012) 12924–12927.
[31] T. Iwai, R. Murakami, T. Harada, S. Kawamorita, M. Sawamura, Adv. Synth. Catal. 356 (2014) 1563–1570.
[32] F. Wu, Y. Feng, C.W. Jones, ACS Catal. 4 (2014) 1365–1375.
[33] M. Waki, Y. Maegawa, K. Hara, et al., J. Am. Chem. Soc. 136 (2014) 4003–4011.
[34] Y. Maegawa, S. Inagaki, Dalton Trans. 44 (2015) 13007–13016.
[35] W.R. Gruening, G. Siddiqi, O.V. Safonova, C. Coperet, Adv. Synth. Catal. 356 (2014) 673–679.
[36] K. Maeda, Y. Uemura, W.J. Chun, et al., ACS Catal. 10 (2020) 14552–14559.
[37] S. Zhang, H. Wang, M. Li, et al., Chem. Sci. 8 (2017) 4489–4496.
[38] A.K. Cook, S.D. Schimler, A.J. Matzger, M.S. Sanford, Science 351 (2016) 1421–1424.
[39] K.T. Smith, S. Berritt, M. Gonzalez-Moreiras, et al., Science 351 (2016) 1424–1427.
[40] O. Staples, M.S. Ferrandon, G.P. Laurent, et al., J. Am. Chem. Soc. 145 (2023) 7992–8000.
[41] A. Prakash, S. Saini, S. Basappa, et al., ChemCatChem 15 (2023) e202201156.
[42] K. Manna, T. Zhang, W. Lin, J. Am. Chem. Soc. 136 (2014) 6566–6569.
[43] K. Manna, T. Zhang, F.X. Greene, W. Lin, J. Am. Chem. Soc. 137 (2015) 2665–2673.
[44] T. Sawano, Z. Lin, D. Boures, et al., J. Am. Chem. Soc. 138 (2016) 9783–9786.
[45] X. Feng, Y. Song, Z. Li, et al., J. Am. Chem. Soc. 141 (2019) 11196–11203.
[46] T. Zhang, K. Manna, W. Lin, J. Am. Chem. Soc. 138 (2016) 3241–3249.
[47] K. Manna, P. Ji, Z. Lin, et al., Nat. Commun. 7 (2016) 12610.
[48] M.I. Gonzalez, E.D. Bloch, J.A. Mason, S.J. Teat, J.R. Long, Inorg. Chem. 54 (2015) 2995–3005.
[49] X. Zhang, Z. Huang, M. Ferrandon, et al., Nat. Catal. 1 (2018) 356–362.
[50] Z.H. Syed, Z. Chen, K.B. Idrees, et al., Organometallics 39 (2020) 1123–1133.
[51] S. Leubner, H. Zhao, N. Van Velthoven, et al., Angew. Chem. Int. Ed. 58 (2019) 10995–11000.
[52] Y. Zhang, J. Li, X. Yang, et al., Chem. Commun. 55 (2019) 2023–2026.
[53] R. Newar, W. Begum, N. Antil, et al., Inorg. Chem. 59 (2020) 10473–10481.
[54] R. Newar, W. Begum, N. Akhtar, et al., Eur. J. Inorg. Chem. 2022 (2022) e202101019.
[55] R. Kalita, M. Chauhan, P. Gupta, et al., Chem. Commun. 60 (2024) 6504–6507.
[56] Z. Zhuang, Y. Wang, Z. Chen, et al., Mater. Chem. Front. 4 (2020) 1158–1163.
[57] A. Dhakshinamoorthy, C.V. Garcia, P. Concepcion, H. Garcia, Catal. Today 366 (2021) 212–217.
[58] J. Chen, H. Li, H. Wang, et al., Chem. Commun. 59 (2023) 8432–8435.
[59] S. Basappa, A. Prakash, S.S. Talekar, M.V. Mane, S.K. Bose, ACS Catal. 14 (2024) 3065–3073.
[60] X. Wu, X. Han, Y. Liu, Y. Liu, Y. Cui, J. Am. Chem. Soc. 140 (2018) 16124–16133.
[61] N. Tahir, F. Muniz-Miranda, J. Everaert, et al., J. Catal. 371 (2019) 135–143.
[62] H. Vardhan, Y. Pan, Z. Yang, et al., APL Mater. 7 (2019) 101111.
[63] J.H. Kim, T. Constantin, M. Simonetti, et al., Nature 595 (2021) 677.

[64] A. Basak, S. Karak, R. Banerjee, J. Am. Chem. Soc. 145 (2023) 7592–7599.
[65] M.A. Legare, M.A. Courtemanche, E. Rochette, F.G. Fontaine, Science 349 (2015) 513–516.
[66] M.A. Legare, E. Rochette, J. Legare Lavergne, N. Bouchard, F.G. Fontaine, Chem. Commun. 52 (2016) 5387–5390.
[67] N. Bouchard, F.G. Fontaine, Dalton Trans. 48 (2019) 4846–4856.
[68] N.R. Bennedsen, F. Yang, F. Goodarzi, S. Kramer, S. Kegnaes, Top. Catal. 66 (2023) 1451–1456.
[69] T.J. Mazzacano, N.P. Mankad, ACS Catal. 7 (2017) 146–149.
[70] D. Yoshii, X. Jin, N. Mizuno, K. Yamaguchi, ACS Catal. 9 (2019) 3011–3016.
[71] D. Yoshii, T. Yatabe, T. Yabe, K. Yamaguchi, ACS Catal. 11 (2021) 2150–2155.
[72] Y. Li, U. Kanbur, J. Cui, et al., Angew. Chem. Int. Ed. 61 (2022) e202117394.
[73] P.K. Verma, M.L. Shegavi, S.K. Bose, K. Geetharani, Org. Biomol. Chem. 16 (2018) 857–873.
[74] Y. Zhu, C. Koh, A.T. Peng, et al., Inorg. Chem. 47 (2008) 5756–5761.
[75] G. Yan, Y. Jiang, C. Kuang, et al., Chem. Commun. 46 (2010) 3170–3172.
[76] S. Kawamorita, H. Ohmiya, T. Iwai, M. Sawamura, Angew. Chem. Int. Ed. 50 (2011) 8363–8366.
[77] A. Bej, D. Srimani, A. Sarkar, Green Chem. 14 (2012) 661–667.
[78] V. Pandarus, O. Marion, G. Gingras, et al., ChemCatChem 6 (2014) 1340–1348.
[79] V. Pandarus, G. Gingras, F. Beland, R. Ciriminna, M. Pagliaro, Org. Process Res. Dev. 18 (2014) 1556–1559.
[80] Z.F. Jiao, J.X. Zhao, X.N. Guo, X.Y. Guo, Chin. J. Catal. 41 (2020) 357–363.
[81] J.H. Kim, Y.K. Chung, RSC Adv. 4 (2014) 39755–39758.
[82] X.F. Zhou, Y.D. Wu, J.J. Dai, et al., RSC Adv. 5 (2015) 46672–46676.
[83] M.L. Shegavi, A. Agarwal, S.K. Bose, Green Chem. 22 (2020) 2799–2803.
[84] S. Saini, D.S. Gavali, R. Bhawar, et al., Catal. Sci. Technol. 13 (2023) 147–156.
[85] M. Franco, R. Sainz, A.M. Lamsabhi, et al., Catal. Sci. Technol. 11 (2021) 3501–3513.
[86] B. Mohan, H. Kang, K.H. Park, Catal. Commun. 85 (2016) 61–65.
[87] D. Annas, S.A. Hira, S. Song, et al., RSC Adv. 11 (2021) 32965–32972.
[88] Z.F. Jiao, Y.M. Tian, X.N. Guo, et al., J. Catal. 395 (2021) 258–265.
[89] P. Zhang, I.A. Roundtree, J.P. Morken, Org. Lett. 14 (2012) 1416–1419.
[90] H. Miura, Y. Hachiya, H. Nishio, et al., ACS Catal. 11 (2021) 758–766.
[91] H. Miura, M. Doi, Y. Yasui, et al., J. Am. Chem. Soc. 145 (2023) 4613–4625.
[92] H. Miura, Y. Yasui, Y. Masaki, M. Doi, T. Shishido, ACS Catal. 13 (2023) 6787–6794.
[93] M. Doi, H. Miura, T. Shishido, Org. Lett. 26 (2024) 2902–2907.
[94] Y. Fan, D.W. Kang, S. Labalme, J. Li, W. Lin, Angew. Chem. Int. Ed. 62 (2023) e202218908.
[95] A. Prakash, S. Basappa, B. Jeebula, et al., Org. Lett. 26 (2024) 2569–2573.
[96] P. Shang, X. Yan, Y. Li, et al., Chin. Chem. Lett. 34 (2023) 107584.